Int. J. Heat Mass Transfer. Vol. 28, No. 9, pp. 1733–1745, 1985
Printed in Great Britain

0017-9310/85 $3.00 + 0.00
Pergamon Press Ltd.

Free convection heat transfer from vertical and horizontal short plates

M. MIYAMOTO, Y. KATOH, J. KURIMA, S. KURIHARA and K. YAMASHITA
Department of Mechanical Engineering, Yamaguchi University, Ube, Japan

(*Received* 12 *October* 1984 *and in final form* 28 *January* 1985)

Abstract—Free convection heat transfer from vertical and horizontal short plates was numerically analyzed by the finite-difference method. The present results regarding average Nusselt number on vertical and horizontal thin plates can be closely approximated by the following equation:

Vertical thin plate,

$$\overline{Nul} = 0.448 + 0.46 Grl^{1/4}, \quad Pr = 0.72 \text{ and } 15 \leqslant Grl \leqslant 27{,}000.$$

Horizontal thin plate,

$$\overline{Nuld} = 0.353 + 0.509 Grd^{1/5}, \quad Pr = 0.72 \text{ and } 4 \leqslant Grd \leqslant 27{,}000.$$

These relations between Nusselt and Grashof numbers show the same tendency as the experimental results and give slightly lower Nusselt numbers. The average Nusselt numbers on the vertical plate (height = l) with finite thickness (d) can be approximated by the above correlation for a thin vertical plate with an error within about 6% using characteristic length $l+d$ in both Nusselt and Grashof numbers instead of l, in the range of $L \geqslant 5$ and $D \leqslant 10$. Where L is dimensionless plate height and D is dimensionless plate thickness.

1. INTRODUCTION

IN THE REGION of Grashof number smaller than 10^5, free convection heat transfer around a horizontal circular cylinder and a sphere has been studied by many investigators. On the other hand, in this range of Grashof number little has been published about free convection around a vertical plate or a horizontal plate, which is one of the fundamental configurations for the heat transfer science other than horizontal cylinders and spheres. In particular, a short vertical plate is of practical use because of its higher heat transfer coefficient of free convection. In order to contribute to the free convection cooling of electronic elements, which have been rapidly miniaturized in recent years and many of which are supersensitive for the surroundings temperature, the study of free convection heat transfer around these short plates, including horizontal plates becomes practically important.

Saunders [1] experimentally studied the free convection heat transfer to air from a vertical short plate in this smaller Grashof number region. McAdams [2] proposed a correlation curve giving the relation between an average Nusselt number and a Rayleigh number of the free convection from a vertical short plate, which was based on the Saunders' experimental results. On the other hand, it was indicated by Fujii [3] and Ede [4] that the heat transfer coefficients obtained experimentally usually had a tendency to be higher than the theoretical solution, because of the difficulty of accurately estimating the other large heat losses and because of various other sources. They also pointed out that the property values quoted by Saunders were not very accurate. Hence McAdams' correlation [2] gives a higher average Nusselt number than the Saunders experimental results re-evaluated by using the latest data of the physical properties.

Suriano and Yang [5] obtained the finite-difference solutions of Navier–Stokes and energy equations for the free convection around vertical and horizontal plates in the region of Rayleigh number smaller than 300; but, regarding the relation between average Nusselt number and Rayleigh number, their numerical results showed a different tendency from that shown by Saunders' experimental results. Recently Martynenko *et al.* [6] obtained the asymptotic solutions of Navier–Stokes and energy equations for a short vertical plate considering the higher-order effects of leading and trailing edges on the boundary-layer solution. They compared their results of the average Nusselt number with the experimental results rearranged by Ede [4]. (However the experimental data plotted on the figure in Martynenko's paper is in part different from the data in Ede's original figure.) It seems that their results are approximately in accord with McAdams' correlation. Noto and Matsumoto [7] carried out a three-dimensional numerical analysis of free convection around a vertical plate of short height and narrow width.

On the other hand, there are a few publications about free convection from a horizontal plate in the Grashof number region smaller than 10^5, particularly in the area where the top and bottom surfaces of the horizontal plate are simultaneously immersed in the fluid and the free convections from both surfaces are allowed to interfere with each other. Fujita *et al.* [8] measured the average Nusselt numbers of the free convection on an inclined plate including the vertical and horizontal

NOMENCLATURE

As	aspect ratio, d/l
d	horizontal length (width) of cross section of rectangular prism
D	dimensionless form of d, defined by equations (4) and (5)
g	acceleration due to gravity
Gr, Grd	Grashof number, D^3
Grl	Grashof number, L^3
Grx	Grashof number, X^3, for uniform temperature rectangular prism, equation (4)
Grx^*	modified Grashof number, X^4, for vertical plate with uniform surface heat flux, equation (5)
h_1	distance between leading edge of the plate and horizontal floor
h_2	distance between ceiling and trailing edge of the plate
H_1, H_2	dimensionless forms of h_1 and h_2, equations (4) and (5)
l	vertical length of cross section of rectangular prism
l'	characteristic length evaluated by King's rule
L	dimensionless form of l, equations (4) and (5)
n	normal distance from surfaces of rectangular prism
N	dimensionless form of n, equation (4)
Nud	local Nusselt numbers on bottom and top horizontal surfaces of rectangular prism, equation (14)
$\overline{Nul}$	average Nusselt number on rectangular prism, defined by cquations (16) and (18)
$\overline{Nuld}$	average Nusselt number on rectangular prism, defined by equation (17), $\overline{Nul}(L+D)/L$
Nux	local Nusselt number on vertical surface, equation (13)
$Nuy0, Nuyl$	local Nusselt numbers on bottom and top horizontal surfaces of rectangular prism
qw	surface heat flux
t	time
T, T_∞	temperature and ambient temperature
Tw	temperature on surfaces of rectangular prism
u, v	velocity in x and y directions
U, V	dimensionless forms of u and v, equations (4) and (5)
x	vertical distance from leading edge of vertical plate
y	horizontal distance from vertical center line of the plate
X, Y	dimensionless forms of x and y, equations (4) and (5).

Greek symbols

$\alpha, \bar{\alpha}$	local and average heat transfer coefficients, equations (13)–(15)
β	volume expansion
ΔT	temperature difference, equation (4)
ζ	vorticity, $\partial v/\partial x - \partial u/\partial y$
θ	dimensionless temperature difference, equations (4) and (5)
λ	thermal conductivity
ν	kinematic viscosity
ξ	dimensionless vorticity, equations (4) and (5)
τ	dimensionless time, equations (4) and (5)
ϕ	stream function, $u = \partial\phi/\partial y$, $v = -\partial\phi/\partial x$
ψ	dimensionless stream function, equations (4) and (5).

plates by using a horizontally stretched ribbon. Their experimental results regarding average Nusselt number on the vertical plate were slightly lower than Saunders' experimental results. Their results on the horizontal plate had a different outcome than the theoretical solutions obtained by Suriano and Yang.

In this paper, the free convection heat transfer around the vertical and horizontal plates was analyzed theoretically by using the finite-difference solutions of the Navier–Stokes and other energy equations. In order to investigate the effects of thickness of the vertical and horizontal plates on the free convection heat transfer, the free convection around the rectangular prisms, which was constructed of only horizontal and vertical surfaces, was analyzed by the same finite-difference method. On the basis of numerical solutions for various aspect ratios (aspect ratio is defined by the equation $As = d/l$, where d is horizontal length of prism cross section, l is vertical length of it. $As = 0$ for a vertical thin plate, and $As = \infty$ for a horizontal thin plate), the characteristic length used in the correlation equation involving free convection heat transfer around rectangular prisms was investigated. Sparrow and Ansari [9] experimentally tested the rules for evaluating a characteristic length proposed by King [10] and Lienhard [11]. The

present numerical solution indicates that the Lienhard's rule was useful for free convection heat transfer around rectangular prisms only under limited conditions. Furthermore, the effect of a horizontal ceiling over the vertical plate was numerically studied.

The appropriateness of the present numerical solutions was examined by comparing average Nusselt number on the vertical and horizontal plates and the velocity distributions near the trailing edge of a vertical plate with the previous experimental results. In previous studies [12, 13], which the numerical analysis of free convection around a semi-infinite vertical plate with finite thickness had been carried out using the same finite-difference method as the present method, the numerical results of the velocity fields near the leading edge had been compared with the experimental results. It had been indicated by these studies that the present numerical method had given reasonable solutions near the leading edge. Hence it was demonstrated that the present numerical method gave a reasonable solution concerning the average Nusselt number but also the local distributions of the velocity and temperature in all parts of the entire calculated region for the free convection around a vertical plate. It is impossible to compare the present velocity distributions around a rectangular prism and horizontal plate with experimental results because no experimental study exists; but it is reasonable to suppose that the present numerical solutions for rectangular prism and horizontal plate are appropriate in all parts of the entire calculated region. However at the maximum values of dimensionless height L and width D of a rectangular prism in the present calculations, separation bubbles appeared on the top horizontal surface in the calculated streamline pattern. It seems that these separation bubbles suggest the unstable flow above the top surface, which means the limit of the present numerical analysis (namely the maximum limit of L and D).

2. BASIC EQUATIONS AND NUMERICAL SOLUTIONS

A rectangular prism and coordinate system are shown in Fig. 1. The basic equations which govern the two-dimensional laminar free convection are the equations of energy, vorticity and the relation between vorticity and stream function. These equations are written as the following dimensionless form, using Boussinesq approximation,

$$\frac{\partial\theta}{\partial\tau}=-\frac{\partial U\theta}{\partial X}-\frac{\partial V\theta}{\partial Y}+\frac{1}{Pr}\nabla^2\theta \tag{1}$$

$$\frac{\partial\xi}{\partial\tau}=-\frac{\partial U\xi}{\partial X}-\frac{\partial V\xi}{\partial Y}+\nabla^2\xi-\frac{\partial\theta}{\partial Y} \tag{2}$$

$$\xi+\nabla^2\psi=0. \tag{3}$$

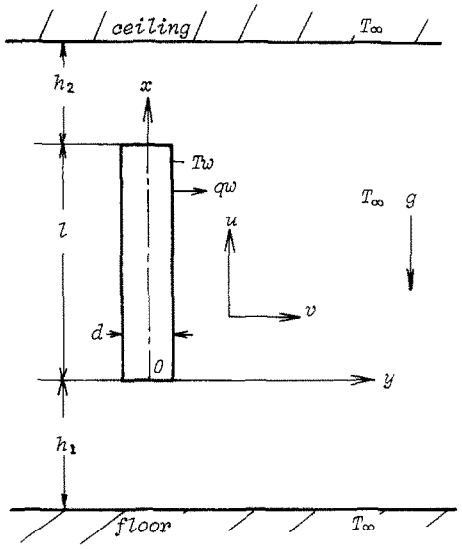

FIG. 1. A rectangular prism and coordinate system.

These dimensionless quantities are defined as follows:

(1) Uniform surface temperature on the rectangular prism

$$\tau=\frac{(g\beta\Delta T)^{2/3}}{\nu^{1/3}}t,\quad X=\left(\frac{g\beta\Delta T}{\nu^2}\right)^{1/3}x,$$

$$U=\frac{u}{(\nu g\beta\Delta T)^{1/3}},\quad \theta=\frac{T-T_\infty}{\Delta T}, \tag{4}$$

$$\Delta T=Tw-T_\infty,\quad \xi=\frac{\nu^{1/3}}{(g\beta\Delta T)^{2/3}}\zeta,\quad \psi=\frac{\phi}{\nu}.$$

(2) Uniform surface heat flux on the vertical plate (being using only in the case of vertical thin plate)

$$\tau=\left(\frac{g\beta qw}{\lambda}\right)^{1/2}t,\quad X=\left(\frac{g\beta qw}{\nu^2\lambda}\right)^{1/4}x,$$

$$U=\left(\frac{\lambda}{g\beta qw\nu^2}\right)^{1/4}u,\quad \theta=\left(\frac{\beta\lambda^3}{\nu^2qw^3}\right)^{1/4}(T-T_\infty), \tag{5}$$

$$\xi=\left(\frac{\lambda}{g\beta qw}\right)^{1/2}\zeta,\quad \psi=\frac{\phi}{\nu}.$$

The dimensionless forms (L, D, Y, H_1, H_2, N) of the physical length (l, d, y, h_1, h_2, n) are defined by the same way as x.

The flow is considered to be symmetric about the vertical center plane of the rectangular prism.

The boundary conditions become

$$U=V=\psi=0,\quad \xi=-\frac{\partial^2\psi}{\partial N^2}$$

and

$$\theta=1,\quad \text{for uniform surface temperature}$$

or

$$-\frac{\partial\theta}{\partial Y}=1,\quad \text{for uniform surface heat flux} \tag{6}$$

on the impermeable rectangular prism,

and

$$\psi = V = \xi = \frac{\partial U}{\partial Y} = \frac{\partial \theta}{\partial Y} = 0 \tag{7}$$

on the symmetry lines.

The following inflow and outflow boundary conditions were used on the outer boundary [14].

$$X = X_{\max}, \quad 0 \leqslant Y \leqslant Y_{\max};$$
$$V = \frac{\partial^2 \psi}{\partial X^2} = \frac{\partial \theta}{\partial X} = 0, \quad \xi = -\frac{\partial^2 \psi}{\partial Y^2} \tag{8}$$

$$X_{\min} \leqslant X \leqslant X_{\max}, \quad Y = Y_{\max};$$
$$U = \frac{\partial^2 \psi}{\partial Y^2} = \theta = 0, \quad \xi = -\frac{\partial^2 \psi}{\partial X^2} \tag{9}$$

$$X = X_{\min}, \quad 0 \leqslant Y \leqslant Y_{\max};$$
$$V = \frac{\partial^2 \psi}{\partial X^2} = \theta = 0, \quad \xi = -\frac{\partial^2 \psi}{\partial Y^2}. \tag{10}$$

When a horizontal floor was placed below the vertical plate, the boundary conditions instead of equation (10) are

$$X = -H_1, \quad 0 \leqslant Y \leqslant Y_{\max};$$
$$U = V = \psi = \theta = 0, \quad \xi = -\frac{\partial^2 \psi}{\partial X^2} \tag{11}$$

on the horizontal floor. When a horizontal ceiling was placed over the vertical plate, the boundary conditions instead of equation (8) are

$$X = H_2, \quad 0 \leqslant Y \leqslant Y_{\max};$$
$$U = V = \psi = \theta = 0, \quad \xi = -\frac{\partial^2 \psi}{\partial X^2} \tag{12}$$

on the horizontal ceiling.

Basic equations (1)–(3) with the above-mentioned boundary conditions were numerically solved by the finite-difference ADI method using a variable mesh size. Further details of the numerical method are given in refs. [12 and 13].

The local Nusselt numbers on the vertical surface are defined by the following equations.

$$Nux = \frac{\alpha x}{\lambda} = -X \left.\frac{\partial \theta}{\partial Y}\right|_{Y=D/2},$$

on the uniform temperature surface,

$$Nux = \frac{\alpha x}{\lambda} = \left.\frac{X}{\theta}\right|_{Y=0},$$

on the uniform heat flux surface. (13)

The local Nusselt numbers on bottom and top horizontal surfaces of the rectangular prism with uniform surface temperature are defined by the following equations.

When the characteristic length is d:

$$Nud = \frac{\alpha d}{\lambda} = D \left.\frac{\partial \theta}{\partial X}\right|_{X=0},$$

on the bottom horizontal surface,

$$Nud = \frac{\alpha d}{\lambda} = -D \left.\frac{\partial \theta}{\partial X}\right|_{X=L},$$

on the top horizontal surface. (14)

When the characteristic length is y:

$$Nuy0 = \frac{\alpha y}{\lambda} = Y \left.\frac{\partial \theta}{\partial X}\right|_{X=0},$$

on the bottom horizontal surface,

$$Nuyl = \frac{\alpha y}{\lambda} = -Y \left.\frac{\partial \theta}{\partial X}\right|_{X=L},$$

on the top horizontal surface. (15)

The average Nusselt numbers on the rectangular prism with uniform surface temperature are defined by the following equations.

When the characteristic length is l:

$$\overline{Nul} = \frac{\bar{\alpha} l}{\lambda} = \frac{L}{L+D}\left\{\int_0^L -\left.\frac{\partial \theta}{\partial Y}\right|_{Y=D/2} \mathrm{d}X + \int_0^{D/2}\left[\left.\frac{\partial \theta}{\partial X}\right|_{X=0} - \left.\frac{\partial \theta}{\partial X}\right|_{X=L}\right]\mathrm{d}Y\right\}. \tag{16}$$

When the characteristic length is $l+d$ instead of l:

$$\overline{Nuld} = \frac{\bar{\alpha}(l+d)}{\lambda} = \int_0^L -\left.\frac{\partial \theta}{\partial Y}\right|_{Y=D/2} \mathrm{d}X + \int_0^{D/2}\left[\left.\frac{\partial \theta}{\partial X}\right|_{X=0} - \left.\frac{\partial \theta}{\partial X}\right|_{X=L}\right]\mathrm{d}Y. \tag{17}$$

The average Nusselt number on the uniform heat flux surface (a vertical surface only) is given by the following equation

$$\overline{Nul} = \frac{\bar{\alpha} l}{\lambda} = \frac{L}{\int_0^L \theta|_{Y=0}\, \mathrm{d}X}. \tag{18}$$

The calculated results in the case of uniform surface heat flux can be transformed to that of uniform surface temperature by following equation

$$Grx^* = Nux\, Grx. \tag{19}$$

3. NUMERICAL RESULTS AND DISCUSSIONS

Numerical solutions were computed on a FACOM M-200 in Kyushu University and an ACOS-800 in Yamaguchi University. The Prandtl number in all computations was 0.72. In the case of the vertical plate with aspect ratio smaller than 1, a horizontal floor was placed under the vertical plate. The dimensionless distance H_1 from the leading edge to the floor was

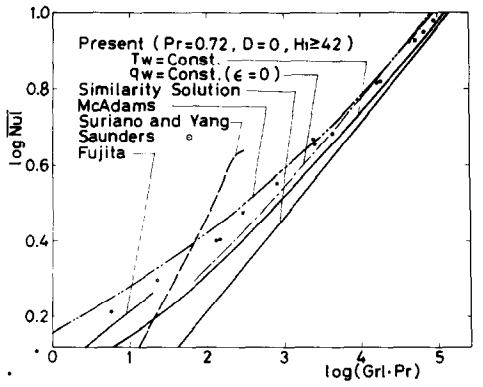

FIG. 2. Comparison of average Nusselt number on a thin vertical plate.

larger than 40. Accordingly, the effects of the floor on the free convection heat transfer were very small. The differences in the local heat transfer coefficient distributions on the vertical plate between $H_1 = 40$ and $H_1 = \infty$ was negligibly small as verified in the previous papers [12, 13]. For the aspect ratio larger than 1, the inflow conditions [given by equation (10)] were used instead of the floor on the bottom boundary ($X = X_{min}$) positioned at the dimensionless distance H_1 of about 40 from the leading edge. When a horizontal ceiling was not placed over the heated plate (most calculations of the present studies were the case), the outflow conditions [given by equation (8)] were used on the upper boundary ($X = X_{max}$) of the calculated region, which was positioned at the dimensionless distance H_2 from the trailing edge. ($H_2 = 20$ for $D = 0$ and $H_2 = 40$ for $D > 0$.)

3.1. *Average Nusselt number on vertical and horizontal thin plates*

Vertical thin plate ($D \simeq 0$). The present numerical results of average Nusselt number for a thin vertical plate are compared with the previous experimental and theoretical results in Fig. 2. The experimental results obtained by Saunders [1] have been re-evaluated by using the latest data of the physical properties at film temperature after the method of Fujii's study [3].

The difference between the re-evaluated Saunders results and those of McAdams (indicated by a two-dotted chain line) can be considered to be caused by the difference of physical properties. The boundary condition on the heated surface in Saunders' experiment seems to be close to the uniform heat flux condition. The present results for the uniform heat flux condition agree well with Saunders' results at larger Rayleigh number ($Grl\ Pr$) than $10^{3.5}$. The present solutions indicate that the difference of $\overline{Nul}$ caused by the difference of the thermal boundary conditions becomes smaller and that the difference between the present theoretical result and Saunders' experimental result becomes larger, while Rayleigh number becomes smaller. The recent experimental results obtained by Fujita *et al.* [8] give a value of $\overline{Nul}$ closer to the present study than that of Saunders'. But in all cases, the experiments give higher $\overline{Nul}$ than the present theoretical solutions at smaller Rayleigh number. The theoretical result obtained by Suriano and Yang [5] have a different tendency from the experimental results. The present result of average Nusselt number on the uniform temperature surface is approximated closely by the following equation.

$$\overline{Nul} = 0.448 + 0.46\ Grl^{1/4}, \qquad Pr = 0.72 \quad \text{and} \quad 15 \leqslant Grl \leqslant 27{,}000. \tag{20}$$

Equation (20) gives slightly smaller Nusselt number than Churchill and Chu correlation [15] given by (21) when

$$Pr = 0.72, \quad \overline{Nul} = 0.68 + 0.475\ Grl^{1/4}. \tag{21}$$

The recently published theoretical solutions obtained by Martynenko *et al.* (not shown in Fig. 2) give approximately the same value as the average Nusselt number recommended by McAdams shown in Fig. 2. They obtained the solutions for $Grl > 20$.

Horizontal thin plate ($L \simeq 0$). The present numerical results of average Nusselt number on the horizontal thin plate are compared with the previous experimental and theoretical results in Fig. 3. The present solutions give the lower average Nusselt number than the experimental results obtained by Fujita *et al.* [8] and Buzunik and Bezlomstev [16] (which was quoted from Suriano and Yang's paper); but the present tendency of the Nusselt–Rayleigh relation bears a close parallel to the experimental results. Suriano and Yang's theoretical solutions give a different tendency of the Nusselt–Rayleigh relation to that in the experimental results. Sugawara and Michiyoshi [17] theoretically studied the free convection heat transfer around the horizontal plate using the boundary-layer approximation and their result of average Nusselt number on the only bottom horizontal surface of the horizontal heated plate is given by equation (22) and in Fig. 3

$$\overline{Nuld} = 0.264\,(Grd\ Pr)^{1/4}. \tag{22}$$

Singh *et al.* [18] obtained theoretically the following correlation equation of average Nusselt number on the downward facing horizontal heated surface using the boundary-layer approximation

$$\overline{Nuld} = 0.5\,(Grd\ Pr)^{1/5}. \tag{23}$$

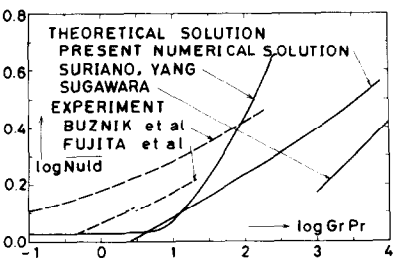

FIG. 3. Comparison of average Nusselt number on a horizontal thin plate.

Table 1. Average Nusselt numbers on vertical and horizontal thin plates

L	D	a $\overline{Nuld}$	b $0.448+0.46\,L^{3/4}$	(a−b)/b (%)
			$0.353+0.509\,D^{3/5}$	
30	0	6.37	6.35	0.4
20	0	4.79	4.80	0.1
10	0	3.00	3.04	−1.2
5	0	1.96	1.99	−1.3
2.5	0	1.41	1.36	3.8
0	1.6	1.02	1.03	−0.5
0	3	1.35	1.34	1.0
0	6	1.83	1.84	−1.0
0	10	2.41	2.38	1.3
0	12	2.58	2.61	−1.4
0	30	4.26	4.27	−0.2

On the other hand, the present numerical result is closely approximated by the following equation obtained by the least-square method,

$$\overline{Nuld} = 0.353+0.509\,Grd^{1/5}, \qquad Pr = 0.72 \quad \text{and} \quad 4 \leqslant Grd \leqslant 27{,}000. \tag{24}$$

It is interesting that Singh's correlation equation is similar to the present numerical solution for horizontal plate.

As mentioned above, the present numerical solutions in the both cases of horizontal and vertical plates give a slightly lower average Nusselt number than in previous experiments. But the present Nusselt–Rayleigh correlations in both cases are practically in parallel with the experimental results. Considering that an experiment of free convection heat transfer generally has a tendency to give a higher heat transfer coefficient [3, 4], it can be concluded that the present numerical solutions give reasonable results on the whole. The present numerical values of the average Nusselt numbers are given in Table 1.

3.2. *Comparison of the velocity distributions near the trailing edge of the vertical plate*

In Fig. 4, the present dimensionless vertical velocity distribution along the X axis above the trailing edge of the vertical thin plate is compared with the experimental results measured by Hardwick and Levy [19] using a hot wire sensor. The ordinate $U/L^{1/2}$ which is equivalent to the similarity variable in the boundary-layer solution is used in Fig. 4 because there is a difference between the plate dimensionless height L in the present numerical solution and in the experiment. The dotted line in Fig. 4 indicates the following result of the similarity solution obtained by Gebhart [20] for the plume rising from a horizontal line heat source

$$\left.\frac{U}{L^{1/2}}\right|_{Y=0} = 0.9\left\{\frac{X-L}{X}\right\}^{1/5}, \qquad Pr = 0.7. \tag{25}$$

Equation (25) was derived from the Gebhart's similarity solution on the assumption that the rate of heat transferred to air from the vertical plate, which is estimated by using the similarity solution of the laminar free convection boundary layer [3], corresponds to the rate of heat generated from the line heat source. As shown in Fig. 4, the present velocity distribution is approximately consistent with the experimental result. It can be supposed that the main cause of the slight difference between the present solution and the experiment is attributed to the difference of dimensionless plate height L.

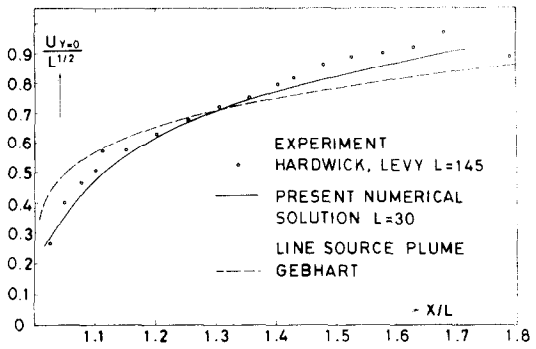

FIG. 4. Comparison of dimensionless vertical velocity distribution along X axis above trailing edge of a vertical plate.

In Fig. 5 the present horizontal distributions of the dimensionless vertical velocity are compared with the same experimental results as in Fig. 4. The similarity variables in the boundary-layer analysis are also used as the coordinate axes in Fig. 5 in order to reduce the influence of the difference of L between the present solution and the experiment. However, the influence of difference between the present dimensionless plate height and the experimental one cannot be eliminated completely even by using the similarity variables. Strictly speaking, the boundary-layer approximation cannot be used in this flow region near the trailing edge. Figure 5 shows that the present velocity distributions

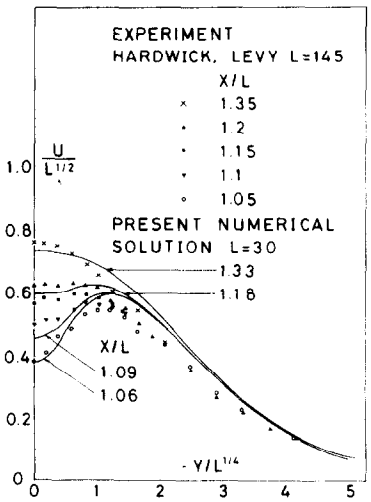

FIG. 5. Comparison of horizontal distributions of dimensionless vertical velocity above trailing edge of a vertical plate.

roughly agree with the experimental results in spite of the difference of L. After all it appears that the present numerical analysis gives a reasonable solution near the trailing edge of the vertical plate. Furthermore, considering the previous investigations [12, 13] of the free convection heat transfer near the leading edge of the semi-infinite vertical plate, it can be concluded that the present numerical analysis gives a reasonable solution in all parts of the entire calculated region around the vertical plate.

3.3 *Average Nusselt number on the horizontal rectangular prism and its characteristic length*

For the vertical plates with various dimensionless heights L and various dimensionless thickness D (which means a rectangular prism $l \times d$), the average Nusselt numbers computed from the finite-difference solutions are tabulated in columns $\overline{Nul}$ and $\overline{Nuld}$ of Table 2. $\overline{Nul}$ and $\overline{Nuld}$, as defined by equations (16) and (17) respectively, indicate the average Nusselt numbers computed from each finite-difference solution, using l and $l+d$ respectively, as the characteristic length. The value of $\overline{Nul}$ is reduced as D increases with constant L, as shown in Table 2, because the average heat transfer coefficient is reduced as the dimensionless thickness D increases with constant L. On the other hand, on contrast with $\overline{Nul}$, $\overline{Nuld}$ increases in spite of decrease of the heat transfer coefficient as D increases with constant L because of its characteristic length $l+d$. The numerical values in column b of Table 2 indicate the average Nusselt numbers estimated from the correlation (20) using the corresponding $l+d$ instead of l as the characteristic length in Grashof number. In the final column, the relative difference between $\overline{Nuld}$ and the estimated values in column b are tabulated in a percentage form. These relative differences are smaller than 6% for D lower than 10 excepting $L = 1$ and 2. These facts show that the average Nusselt number on the vertical plate with finite thickness d (horizontal rectangular prism $l \times d$) can be estimated from the correlation equation (20) for the vertical thin plate ($d = 0$) by using $l+d$ as the characteristic length in Nusselt and Grashof numbers. This estimated Nusselt number has an error smaller than 6% for $L \geqslant 5$ and $D \leqslant 10$ regardless of aspect ratio.

Table 2. Average Nusselt numbers on the rectangular prism

L	D	D/L	$\overline{Nul}$	a $\overline{Nuld}$	b $0.448+0.46(L+D)^{3/4}$	(a−b)/b (%)
30	2	0.0677	6.36	6.78	6.64	2
30	6	0.2	6.06	7.27	7.21	1
30	10	0.333	5.72	7.63	7.76	−2
20	2	0.1	4.76	5.23	5.12	2
20	6	0.3	4.43	5.76	5.74	0
20	10	0.5	4.10	6.15	6.34	−3
20	20	1.0	3.53	7.06	7.76	−9
10	2	0.2	2.92	3.50	3.41	3
10	6	0.6	2.56	4.09	4.13	−1
10	10	1.0	2.27	4.53	4.80	−6
10	20	2.0	1.86	5.58	6.35	−12
5	2	0.4	1.82	2.54	2.43	5
5	6	1.2	1.44	3.16	3.23	−2
5	10	2.0	1.26	3.77	3.95	−5
5	20	4.0	0.949	4.75	5.59	−15
2.5	4	1.6	0.893	2.32	2.32	0
2	10	5.0	0.517	3.10	3.41	−9
2	20	10.0	0.375	4.13	5.12	−19
2	30	15.0	0.318	5.09	6.64	−23
1	6	6.0	0.317	2.22	2.28	−3
1	10	10.0	0.249	2.74	3.27	−16
1	20	20.0	0.181	3.80	5.00	−24

These relationships are shown also in graphical form on Fig. 6. In this figure, each symbol indicates the average Nusselt number computed from the present finite-difference solutions for the given constant value of L. Each dotted line indicates that D is constant along it. When the characteristic length is l (indicated by the upper group of lines), average Nusselt numbers ($\overline{Nul}$) for finite values of D are reduced and come to differ considerably from the correlation curve for $D = 0$ (indicated by the solid line) as D increases. On the other hand, when the characteristic length is $l+d$ (indicated by the lower group of lines), average Nusselt numbers ($\overline{Nuld}$) for finite values of D are not so different from the correlation curve for $D = 0$ in comparison with the case of characteristic length l, even if D increases. The average Nusselt number on a horizontal thin plate ($L = 0$) is indicated, for reference, by dotted chain line.

The characteristic length $l+d$ is the same with the length of travel of boundary layer proposed by Lienhard [11] within the limit of the possibility of the boundary-layer approximation. Sparrow and Ansari [9] pointed out on the basis of their accurate

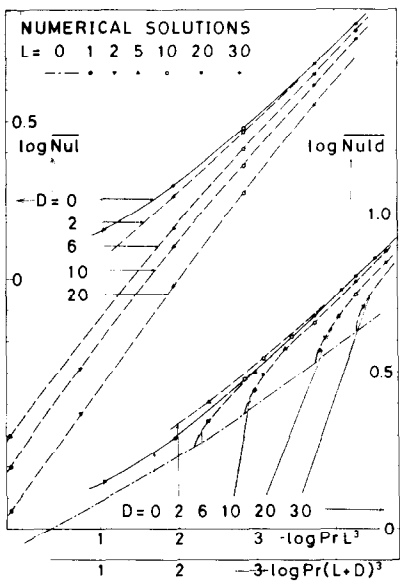

FIG. 6. Comparison of average Nusselt number on a rectangular prism between characteristic length of l and $l+d$.

experimental test that the rules for evaluating a characteristic length of laminar free convection proposed by King and Lienhard are not so effective. But the characteristic length proposed by Lienhard seems to be effective at least for the rectangular prism alone as mentioned above.

In the next place the applicability of King's rule to the rectangular prism will be considered, although King [10] himself did not state that his rule could be used for the rectangular prism. Correlation (20) for thin vertical plate ($d = 0$) gives the following relation between average heat transfer coefficient and characteristic length, neglecting the first term in the RHS of (20)

$$\bar{\alpha} \sim (\text{characteristic length})^{-1/4}. \qquad (26)$$

Equation (26) demonstrates that the larger characteristic length gives the lower heat transfer coefficient. The present finite-difference solutions for the rectangular prism showed that the heat transfer coefficient on the vertical plate with finite thickness d was reduced as its dimensionless thickness D increased and its dimensionless height L was constant, as shown in Table 2. Hence, if the correlation (20) for a thin vertical plate is used to estimate the heat transfer coefficient on the vertical plate with finite thickness, the larger characteristic length than l, such as $l + d$, is adequate to give the lower heat transfer coefficient caused by the finite thickness d.

On the other hand, King's rule ($1/l' = 1/l + 1/d$) gives a smaller characteristic length l' than either l or d, so that this rule gives the estimation of the higher heat transfer coefficient on the vertical plate with finite thickness than on the thin vertical plate with the same height l. This fact is inconsistent with the present finite-difference solutions that an increase of the thickness of the vertical plate causes the reduction of average heat transfer coefficient on it. Hence King's rule is not effective, at least for the rectangular prism.

Concerning the horizontal plate with width d and finite thickness l (large aspect ratio) if the correlation (24) for the thin horizontal plate ($l = 0$) is used to estimate the heat transfer coefficient on the horizontal plate with finite thickness l, the use of characteristic length $l + d$ cannot give a more accurate estimation of the heat transfer coefficient than simply using d as the characteristic length. The heat transfer coefficient on the horizontal plate with finite thickness l increases with the increase of its thickness l, and the correlation (24) as well as equation (20) gives a lower heat transfer coefficient with the use of the larger characteristic length. The heat transfer coefficient on the horizontal plate with finite thickness is maximum at $3 \sim 4$ of its aspect ratio with constant width D, as calculated from the results shown in Table 2.

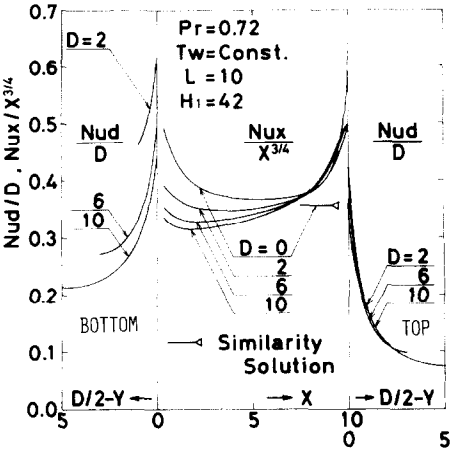

FIG. 7. Local Nusselt number distributions on a short vertical plate with finite thickness, $L = 10$.

3.4. *Local Nusselt number distributions*

The local Nusselt number distributions on the vertical plate with various dimensionless thickness D (0, 2, 6 and 10) and the same dimensionless vertical length (10 or 30) are compared in Figs. 7 and 8, respectively. The distributions shown in the left- and right-hand sides of each figure correspond to the local Nusselt

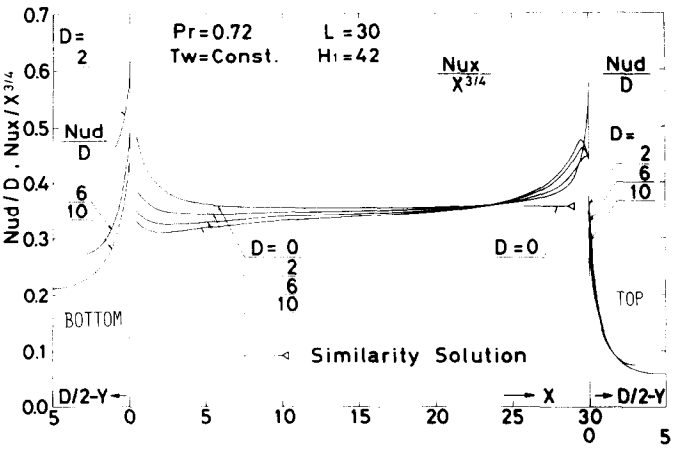

FIG. 8. Local Nusselt number distributions on a short vertical plate with finite thickness, $L = 30$.

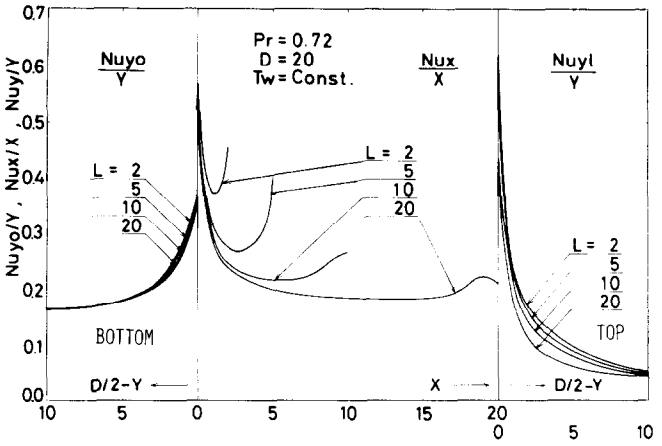

FIG. 9. Local Nusselt number distributions on a short horizontal plate with finite thickness, $D = 20$.

numbers on the bottom and top horizontal surfaces of the thick vertical plate, respectively; but the ordinate for the horizontal surfaces in Figs. 7 and 8 is equivalent to the local Nusselt number divided by D and proportional to the local heat transfer coefficient regardless of the characteristic length in Nusselt number. The local Nusselt numbers on the vertical surface (shown in the central part of each figure) are divided by $X^{3/4}$ to be compared with the similarity solution of the vertical boundary layer. The local heat transfer coefficients on the bottom horizontal surface are larger than those on the corresponding upper horizontal surfaces, as shown in the figures. Each figure indicates that the larger D of the vertical plate with the constant L gives the lower local heat transfer coefficient on its bottom surface and on the lower part of its vertical surface. The local heat transfer coefficient on its top surface and on the upper part of its vertical surface are hardly influenced by the change of D. Furthermore, comparison between these two figures indicates that the local heat transfer coefficients on the bottom surface and the lower part of the vertical surface are almost unaltered by the change of L, if the plate dimensionless thickness D is constant. When D is larger than 2, the local Nusselt numbers on the vertical surface become in part lower than the similarity solution [3].

The local Nusselt number distributions on the horizontal plates with various finite dimensionless thickness L and a constant width D are shown in Fig. 9. In Fig. 9, the local Nusselt numbers on the top and bottom horizontal surfaces are defined by a different characteristic length from that in Figs. 7 and 8; but the ordinates in Fig. 9, which indicate the local Nusselt number divided by Y for horizontal surfaces and the local Nusselt number divided by X for the vertical surface, have the same content with the ordinate for horizontal surface in Figs. 7 and 8, and are proportional to the local heat transfer coefficient regardless of the characteristic length. Figure 9 shows that the local heat transfer coefficient on the bottom horizontal surface is unchanged with the increase of L, but on the top horizontal surface, including the upper part of vertical surface, it shows that the local heat transfer coefficient lowers with the increase of L.

3.5. *The effects of the horizontal ceiling on the free convection heat transfer around the vertical plate*

In Fig. 10 the local Nusselt number distributions on the thin vertical plate ($L = 20$ and $D = 0$) are shown, when the horizontal ceiling over the plate is placed at the various heights from the trailing edge of the plate. At the right-hand side in Fig. 10 average Nusselt numbers are plotted by the broken lines. All these Nusselt numbers are divided by $X^{3/4}$ or $L^{3/4}$ and are to be compared with the similarity solution of the free convection vertical boundary layer. The smaller value of H_2, which is the dimensionless height of the ceiling from the top of the plate, gives the lower Nusselt number. The local Nusselt number distribution very near the leading edge is hardly reduced by a decreasing of H_2. The average and local Nusselt numbers for $H_2 = 20$ are close to these on the vertical plate without a ceiling. For $H_2 = 2$, the local Nusselt number very near the trailing edge becomes very large by the heat conduction because the trailing edge at temperature Tw approaches closely to the ceiling at temperature T_∞.

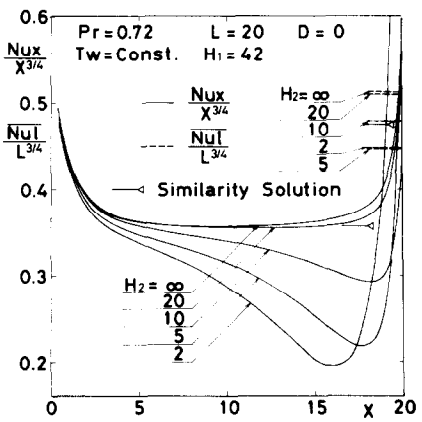

FIG. 10. Nusselt numbers on a thin vertical plate under a horizontal ceiling.

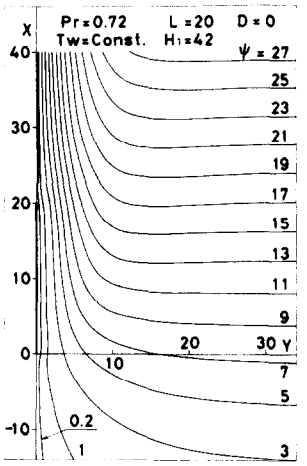

FIG. 11. Distribution of streamline around a thin vertical plate.

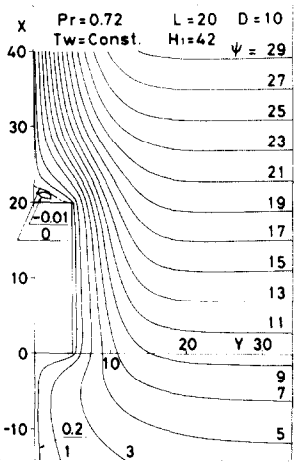

FIG. 13. Distribution of streamline around a rectangular prism.

3.6. *Velocity and temperature fields around vertical and horizontal plates*

The typical patterns of streamline and isotherm lines in the present calculations are shown in the following figures. The distributions of streamline and isothermal line around a vertical thin plate ($L = 20$ and $D = 0$) are shown in Figs. 11 and 12. The streamline pattern under the leading edge indicates that a flow is drawn into the sink at the leading edge. When $L = 20$ and $D = 10$, these distributions are shown in Figs. 13 and 14. There is a small separation bubble on the top surface of the plate. This separation bubble disappears in the case of the shorter vertical plate with the same thickness ($L = 10$ and $D = 10$). The distributions of streamline and isotherm lines around a horizontal thin plate are shown in Figs. 15 and 16 ($L = 0$ and $D = 30$). There are two small separation bubbles on the top surface of the plate. These separation bubbles disappear in the case of the thicker horizontal plate with the same width ($L = 2$ and $D = 30$). It seems that these separation bubbles suggest the possibility of unstableness and asymmetry of the flow above the top horizontal surface for larger values of D and L, which mean the limit of the present numerical analysis.

4. CONCLUSIONS

(1) The present results regarding average Nusselt numbers on vertical and horizontal thin plates can be closely approximated by the following equations:

vertical thin plate

$$\overline{Nul} = 0.448 + 0.46\, Grl^{1/4},$$

$$Pr = 0.72 \quad \text{and} \quad 15 < Grl < 27{,}000;$$

horizontal thin plate

$$\overline{Nuld} = 0.353 + 0.509\, Grd^{1/5},$$

$$Pr = 0.72 \quad \text{and} \quad 4 < Grd < 27{,}000.$$

(2) These Nusselt–Grashof relations show the same tendency as the corresponding experimental results

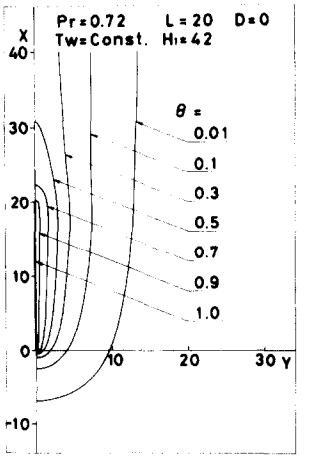

FIG. 12. Distribution of isothermal line around a thin vertical plate.

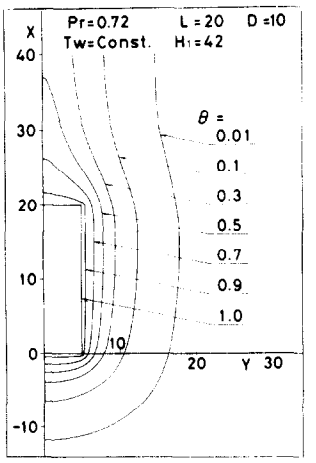

FIG. 14. Distribution of isothermal line around a rectangular prism.

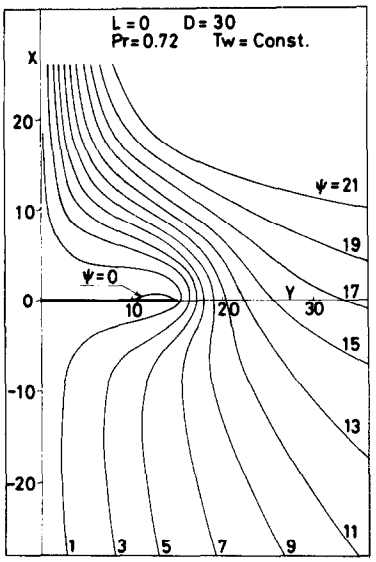

FIG. 15. Distribution of streamline around a thin horozintal plate.

and give slightly lower Nusselt number than the experimental results.

(3) The present results of the velocity distributions near the trailing edge of the vertical plate approximately agree with the experimental results.

(4) These facts together with the previous investigations of free convection near the leading edge of the semi-infinite vertical plate indicate that the present numerical analysis gives a reasonable solution concerning the free convection around vertical and horizontal plates regarding not only the average heat transfer rate but also the local distributions of the velocity and temperature.

(5) When the dimensionless thickness D of the vertical plate increases with the constant dimensionless height L, the average heat transfer coefficient on it decreases, and the local heat transfer coefficients on the bottom horizontal surface and the lower vertical surface decrease more severely than on the other surfaces.

(6) When the dimensionless thickness L of the horizontal plate increases with the constant dimensionless width D, the average heat transfer coefficient on it is maximum at its aspect ratio of approximately $3 \sim 4$, and the local heat transfer coefficient on the top horizontal surface decreases more severely than on the bottom horizontal surface.

(7) The local heat transfer coefficient is higher on the bottom horizontal surface than on the top horizontal surface of the rectangular prism.

(8) In the range of $L \geqslant 5$ and $D \leqslant 10$, using length $l+d$ as the characteristic length in both Nusselt and Grashof numbers instead of l or d, average Nusselt numbers on the vertical plate with finite thickness d can be approximated by the correlation equation (20) for the vertical thin plate ($d = 0$) with an error within 6%.

(9) The effects of the ceiling over the plate on the free convection heat transfer is negligibly small at the larger dimensionless height H_2 of the ceiling from the plate trailing edge than 20, when L is 20 and D is 0.

(10) There is a separation bubble on the top horizontal surface of the rectangular prism for $L \geqslant 20$, $D \geqslant 6$ and $L = 0$, $D = 30$ in the present calculations.

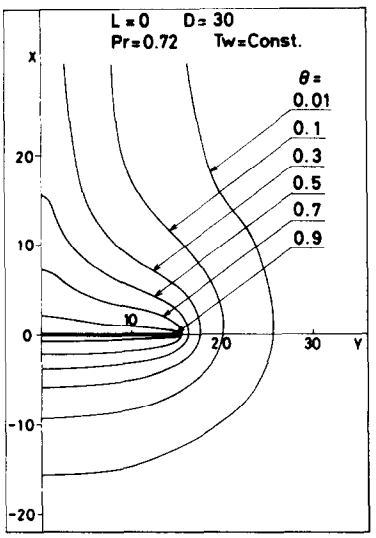

FIG. 16. Distribution of isothermal line around a thin horizontal plate.

REFERENCES

1. O. A. Saunders, Effect of pressure upon natural convection in air, *Proc. R. Soc.* **A157**, 278–291 (1936).
2. W. H. McAdams, *Heat Transmission*. McGraw-Hill, New York (1954).
3. T. Fujii, A grounding of free convection heat transfer. In *Dennetsu-kogaku no Shinten*, Vol. 3, pp. 1–110 (in Japanese). Yookendo, Tokyo (1974).
4. A. J. Ede, Advances in free convection. In *Advances in Heat Transfer*, Vol. 4, pp. 1–64. Academic Press, New York (1967).
5. F. J. Suriano and K. T. Yang, Laminar free convection about vertical and horizontal plates at small and moderate Grashof numbers, *Int. J. Heat Mass Transfer* **11**, 473–490 (1968).
6. O. G. Martynenko, A. A. Berezovsky and Yu. A. Sokovishin, Laminar free convection from a vertical plate, *Int. J. Heat Mass Transfer* **27**, 869–881 (1984).
7. K. Noto and R. Matsumoto, Three-dimensional analysis of natural convection around a vertical plate of short height and narrow width (in Japanese), *Trans. Jap. Soc. Mech. Engrs* **50**, 453, 1431–1437 (1984).
8. N. Fujita, T. Suzuki and T. Tsubouchi, Free convection heat transfer from a horizontal ribbon wire (in Japanese). *18th National Heat Transfer Symposium of Japan*, pp. 301–303 (1981).
9. E. M. Sparrow and M. A. Ansari, A refutation of King's rule for multidimensional external natural convection, *Int. J. Heat Mass Transfer* **26**, 1357–1364 (1983).
10. W. J. King, The basic laws and data of heat transmission—3. Free convection, *Mech. Engng* **54**, 347–353 (1932).
11. John H. Lienhard, On the commonality of equations for natural convection from immersed bodies, *Int. J. Heat Mass Transfer* **16**, 2121–2123 (1973).
12. M. Miyamoto and T. Akiyoshi, Free convection heat

transfer near leading edge of semi-infinite vertical flat plate with finite thickness (1st report, isothermal flat plate), *Bull. Jap. Soc. Mech. Engrs* **24**, 197, 1945–1952 (1981).
13. M. Miyamoto and T. Akiyoshi, Free convection heat transfer near leading edge of semi-infinite vertical plate (2nd report, uniform heat generation), *Bull. Jap. Soc. Mech. Engrs* **25**, 202, 583–590 (1982).
14. T. H. Kuehn and R. J. Goldstein, Numerical solution to the Navier–Stokes equations for laminar natural convection about a horizontal isothermal circular cylinder, *Int. J. Heat Mass Transfer* **23**, 971–980 (1980).
15. S. W. Churchill and H. S. Chu, Correlation equations for laminar and turbulent free convection from a vertical plate, *Int. J. Heat Mass Transfer* **18**, 1323–1329 (1975).
16. V. M. Buzunik and K. A. Bezlomstev, A generalized equation for the heat exchange of natural and forced convection during external flow about bodies, Izv, Uyssh. Ucheb. Zaved. (2), 68–74 (1960); Ref. Zh. Meckl. (6), Rev. 6V506 (1961).
17. S. Sugawara and I. Michiyoshi, Heat Transfer from a horizontal flat plate by natural convection (in Japanese) *Trans Jap. Soc. Mech. Engrs* **21**, 109, 651–657 (1955).
18. S. H. Singh, R. C. Birkebak and R. M. Drake, Jr., Laminar free convection heat transfer from downward-facing horizontal surfaces of finite dimensions, *Prog. Heat Mass Transfer* **2**, 87–98 (1969).
19. N. E. Hardwick and E. K. Levy, Study of the laminar free convection wake above an isothermal vertical plate, *J. Heat Transfer* **95**, 289–294 (1973).
20. B. Gebhart, *Heat Transfer*. McGraw-Hill, New York (1971).

CONVECTION THERMIQUE NATURELLE POUR DES PLANS VERTICAUX ET HORIZONTAUX COURTS

Résumé—La convection thermique pour des plans verticaux et horizontaux courts est analysée numériquement par la méthode des différences finies. Les résultats relatif au nombre de Nusselt moyen peuvent être approchés correctement par les équations suivantes:

Plan vertical mince:

$$\overline{Nul} = 0{,}448 + 0{,}46\, Grl^{1/4}, \quad Pr = 0{,}72 \text{ et } 15 \leqslant Grl \leqslant 27000.$$

Plan horizontal mince:

$$\overline{Nul} = 0{,}353 + 0{,}509\, Grd^{1/5}, \quad Pr = 0{,}72 \text{ et } 4 \leqslant Grd \leqslant 27000.$$

Ces relations entre les nombres de Grashof et de Nusselt montrent la même tendance que les résultats expérimentaux et elles donnent des nombres de Nusselt légèrement inférieurs. Les nombres de Nusselt moyens sur la plaque vertical (hateur Z) avec une épaisseur finie (d) peuvent être approchés par la formule précédente pour une plaque verticale mince, avec une erreur de 6% environ, en utilisant une longueur $l + d$ caractéristique à la fois dans les nombres de Nusselt et de Grashof, à la place de Z, dans le domaine $Z \geqslant 5$ et $D \leqslant 10$, où L est la hauteur adimensionnelle et D l'épaisseur adimensionnelle.

WÄRMEÜBERGANG BEI FREIER KONVEKTION AN KURZEN SENKRECHTEN UND WAAGERECHTEN PLATTEN

Zusammenfassung—Der Wärmeübergang bei freier Konvektion an kurzen senkrechten und waagerechten Platten wurde mit dem Finite-Differenzen-Verfahren numerisch untersucht. Die vorliegenden Ergebnisse für die mittlere Nusselt-Zahl an senkrechten und waagerechten dünnen Platten lassen sich durch die folgenden Gleichungen gut annähern:

Senkrechte Platte:

$$\overline{Nu_L} = 0{,}448 + 0{,}46\, Gr_L^{1/4}, \quad Pr = 0{,}72 \text{ und } 15 \leqslant Gr_L \leqslant 27000$$

Waagerechte Platte:

$$\overline{Nu_{Ld}} = 0{,}353 + 0{,}509\, Gr_d^{1/5}, \quad Pr = 0{,}72 \text{ und } 4 \leqslant Gr_d \leqslant 27000.$$

Diese Beziehungen zwischen Nusselt- und Grashof-Zahlen zeigen dieselbe Tendenz wie die experimentellen Ergenisse, liefern aber geringfügig niedrigere Nusselt-Zahlen. Die mittleren Nusselt-Zahlen bei der senkrechten Platte (Höhe l) mit endlicher Dicke d können mit der obigen Beziehung für die senkrechte Platte angenähert werden, wenn man Nusselt- und Grashof-Zahl mit der charakteristischen Länge $l + d$ statt l bildet. Der Fehler liegt bei maximal 6% für $L \geqslant 5$ und $D \leqslant 10$, wobei L die dimensionslose Plattenhöhe und D die dimensionslose Plattendicke sind.

СВОБОДНОКОНВЕКТИВНЫЙ ТЕПЛОПЕРЕНОС НА ВЕРТИКАЛЬНОЙ И ГОРИЗОНТАЛЬНОЙ КОРОТКИХ ПЛАСТИНАХ

Аннотация—Методом конечных разностей численно проанализирован свободноконвективный теплоперенос на вертикальной и горизонтальной коротких пластинах. Результаты для среднего числа Нуссельта на вертикальной и горизонтальной тонких пластинах можно хорошо аппроксимировать следующими уравнениями:

вертикальная тонкая пластина—

$\overline{Nul} = 0{,}448 + 0{,}46Grl^{1/4}$, $Pr = 0{,}72$ и $15 \leqslant Grl \leqslant 27000$;

горизонтальная тонкая пластина—

$\overline{Nuld} = 0{,}353 + 0{,}509Grd^{1/5}$, $Pr = 0{,}72$ и $4 \leqslant Grd \leqslant 27000$.

Эти соотношения между числами Грасгофа и Нуссельта проявляют ту же тенденцию, что и экспериментальные данные, и дают несколько меньшие значения чисел Нуссельта. Средние числа Нуссельта на вертикальной пластине (высота = l) конечной толщины (d) можно аппроксимировать приведенными выше выражениями для тонкой вертикальной пластины с погрешностью в пределах около 6%, если использовать вместо l характерную длину $l + d$ как для чисел Нуссельта, так и для чисел Грасгофа в диапазоне $L \geqslant 5$ и $D \leqslant 10$, где L—безразмерная высота пластины, D—ее безразмерная толщина.